Supporting Information

Vascular binding of a pathogen under shear force through mechanistically distinct sequential interactions with host macromolecules

[1,2]Tara J. Moriarty, [2]Meiqing Shi^, [3]Yi-Pin Lin, [1]Rhodaba Ebady, [4]Hong Zhou#, [1]Tanya Odisho, [2]Pierre-Olivier Hardy, [2]Aydan Salman-Dilgimen, [5]Jing Wu†, [5]Eric H. Weening&, [5]Jon T. Skare, [4]Paul Kubes, [3]John Leong and [2]George Chaconas**

[1]Matrix Dynamics Group, Faculty of Dentistry, and Department of Laboratory Medicine and Pathobiology, Faculty of Medicine, University of Toronto, ON M5S 3E2, Canada

[2]Snyder Institute for Chronic Diseases, Departments of Biochemistry & Molecular Biology and Microbiology and Infectious Diseases, University of Calgary, Calgary, AB T2N 4N1, Canada

[3]Department of Molecular Biology and Microbiology, Tufts University School of Medicine, Boston, MA 02114, USA

[4]Snyder Institute for Chronic Diseases, Department of Physiology and Pharmacology, University of Calgary, Calgary, AB T2N 4N1, Canada

[5]Department of Microbial and Molecular Pathogenesis, Texas A&M Health Science Center, Texas A&M University, Bryan, TX 77807, USA

---

^Current address: Veterinary Medicine, University of Maryland, College Park, MD 20742-3711, USA

Current address: Department of Microbiology & Immunology, Nanjing Medical University, Nanjing, JS, P.R.China 210029

†Current address: Department of Veterinary Pathobiology, College of Veterinary Medicine, Texas A&M University, College Station, TX 77843, USA

&Current address: Department of Genetics, University of North Carolina at Chapel Hill, Chapel Hill, NC 27599, USA

---

*Correspondence: chaconas@ucalgary.ca; Phone 1-403-210-9692
or tara.moriarty@utoronto.ca; Phone 1-416-978-6685]

SUPPLEMENTAL INFORMATION:

Video Legends S1 and S2
Tables S1-S4
Figures S1-S4

Video S1: **Spinning disk confocal IVM video footage of GFP-expressing infectious *B. burgdorferi* strain GCB966 (green) interacting with a postcapillary venule of the knee joint vasculature.** The vasculature is counterstained with fluorescent antibody to PECAM-1 (red). Elapsed time is shown at the top right and the scale is at the bottom left. The direction of blood flow is from bottom to top.

Video S2: Spinning disk confocal IVM video footage of GFP-expressing infectious *B. burgdorferi* strain GCB966 (green) interacting with a postcapillary venule of the skin vasculature. The vasculature is counterstained with Texas Red-labelled 70 kDa dextran (red). Elapsed time is shown at the top right and the scale at bottom left. Direction of blood flow is down and to the left.

Table S1: *B. burgdorferi* strains used in this study

Strain number	***Background***	***Description***	***Reference***
GCB705	B31-A	Non-infectious high passage strain transformed with GFP expression plasmid pTM61 (clone 1)	(Moriarty *et al.*, 2008)
GCB706	B31-A	Non-infectious high passage strain transformed with GFP expression plasmid pTM61 (clone 2)	(Moriarty et al., 2008)
GCB726	B31 5A4 NP1	Infectious strain transformed with GFP expression plasmid pTM61 (clone 2)	(Moriarty et al., 2008)
ML23/ pJW201 (GCB966)	B31 derivative ML23	Parental ML23 strain (Seshu *et al.*, 2006) transformed with plasmid pJW201(*PflaB*-GFP/*bbe22)* (Wu *et al.*, 2011)	(Wu et al., 2011)
JS315/ pJW201 (GCB971)	ML23 derivative *bbk32::strR*	ML23-derived *bbk32::strR bbk32* knockout strain (Seshu et al., 2006) transformed with plasmid pJW201(*PflaB*-GFP/*bbe22*) (Wu et al., 2011)	(Wu et al., 2011)
GCB1570	GCB706	Non-infectious GFP-expressing high passage strain transformed with pTM242 and expressing RevA	This study
GCB1574	GCB706	Non-infectious GFP-expressing high passage transformed with pTM244 and expressing BB0347	This study
GCB1586	GCB706	Non-infectious GFP-expressing high passage strain transformed with pTM255 and expressing RevB	This study
GCB1585	GCB706	Non-infectious GFP-expressing high passage strain transformed with pTM257 and expressing full-length BBK32	This study
GCB1580	GCB706	Non-infectious GFP-expressing high passage strain transformed with pTM246 and expressing BBK32 Δ45-68	This study
GCB1583	GCB706	Non-infectious GFP-expressing high passage strain transformed with pTM248 and expressing BBK32 Δ158-182	This study
GCB1587	GCB706	Non-infectious GFP-expressing high passage strain transformed with pTM243 and expressing RevA-FLAG	This study
GCB1589	GCB706	Non-infectious GFP-expressing high passage strain transformed with pTM256 and expressing RevB-FLAG	This study
GCB1590	GCB706	Non-infectious GFP-expressing high passage strain transformed with pTM245 and expressing BB0347-FLAG	This study

Table S2: Constructs used in this study

Plasmid	***E. coli strain***	***Description***	***Reference***
pTM61	GCE1173	**P_{flaB}-driven GFP expression** vector: pTM49 (modified pBSV2g)	(Moriarty et al., 2008)
pJW201		***bbe22/pncA* locus cloned into GFP expression plasmid** cassette cloned into pTM61 (Moriarty et al., 2008) via KpnI (Wu et al., 2011)	(Wu et al., 2011)
pTM242	GCE1865	**P_{flaB}-driven RevA expression** cassette cloned into pCE320 (Eggers *et al.*, 2002) via XhoI/NotI; *PflaB* sequence amplified from pTM61 (Moriarty et al., 2008); *revA* coding sequence amplified from B31 5A4 NP1	This study
pTM244	GCE1867	**P_{flaB}-driven BB0347 expression** cassette cloned into pCE320 (Eggers et al., 2002) via XhoI/NotI; *PflaB* sequence amplified from pTM61 (Moriarty et al., 2008); *bb0347* coding sequence amplified from B31 5A4 NP1	This study
pTM255	GCE1878	**P_{flaB}-driven RevB expression** cassette cloned into pCE320 (Eggers et al., 2002) via XhoI/NotI; *PflaB* sequence amplified from pTM61 (Moriarty et al., 2008); *revB* coding sequence amplified from B31 5A4	This study
pTM257	GCE1880	**$P_{fla}B$-driven BBK32 WT expression** cassette cloned into pCE320 (Eggers et al., 2002) via XhoI/NotI; *PflaB* sequence amplified from pTM61 (Moriarty et al., 2008); *bbk32* coding sequence amplified from pBBK32 (Fischer *et al.*, 2006)	This study
pTM248	GCE1871	**P_{flaB}-driven BBK32Δ158-182 expression** cassette cloned into pCE320 (Eggers et al., 2002) via XhoI/NotI; *PflaB* sequence amplified from pTM61 (Moriarty et al., 2008); *bbk32* Δ158-182 coding sequence amplified from pBBK32QC48 (Lin *et al.*, 2012)	This study
pTM246	GCE1869	**P_{flaB}-driven BBK32Δ45-68 expression** cassette cloned into pCE320 (Eggers et al., 2002) via XhoI/NotI; *PflaB* sequence amplified from pTM61 (Moriarty et al., 2008); *bbk32* Δ45-68 coding sequence amplified from pBBK32QC45 (Lin et al., 2012)	This study
pTM243	GCE1866	**P_{flaB}-driven RevA-FLAG expression** cassette cloned into pCE320 (Eggers et al., 2002) via XhoI/NotI; *PflaB* sequence amplified from pTM61 (Moriarty et al., 2008); *revA* coding sequence amplified from B31 5A4 NP1; *3Xflag* coding sequence amplified from pJL148SPA (Zeghouf *et al.*, 2004)	This study
pTM245	GCE1868	**P_{flaB}-driven BB0347-FLAG expression** cassette cloned into pCE320 (Eggers et al., 2002) via XhoI/NotI; *PflaB* sequence amplified from pTM61 (Moriarty et al., 2008); *bb0347* coding sequence amplified from B31 5A4 NP1; *3Xflag* coding sequence amplified from pJL148SPA (Zeghouf et al., 2004)	This study

Constructs used in this study, *continued*

Plasmid	***E. coli strain***	***Description***	***Reference***
pTM256	GCE1879	**P_{flaB}-driven RevB-FLAG expression** cassette cloned into pCE320 (Eggers et al., 2002) via XhoI/NotI; *PflaB* sequence amplified from pTM61 (Moriarty et al., 2008); *revB* coding sequence amplified from B31 5A4; *3Xflag* coding sequence amplified from pJL148SPA (Zeghouf et al., 2004)	This study
pTM222	GCE1845	qPCR DNA quantification standard plasmid, containing *flaB* sequences	(Lee *et al.*, 2010)
pQC44	pBBK32QC44 (Δ45-68)-DH5α	pBBK32QC44 (Δ45-68)	(Lin et al., 2012)
pQC48	pBBK32QC48 (Δ158-182)-DH5α	pBBK32QC48 (Δ158-182)	(Lin et al., 2012)
pYL146	pQE30-RevA-M15	pQE30-RevA: construct for recombinant expression of RevA	This study
pYL147	pQE30-RevB-M15	pQE30-RevB: construct for recombinant expression of RevB	This study
pYL125	pQE30-BB0347-M15	pQE30-BB0347: construct for recombinant expression of BB0347	This study
pJF51	pMal-c2-BBK32-BL21	pMal-c2-BBK32: construct for recombinant expression of MBP-BBK32	(Fischer et al., 2006)

Table S3: Primers used in this study

Primer	Target	Sequence (5'-3')
B1723	5' end of *PflaB* (with XhoI site) (forward primer)	CTCGAGTGTCTGTCGCCTCTTGTGG
B1662	3' end of *PflaB* fused to 5' end of *bbk32* coding sequence (reverse primer)	CAAATATTTACTTTTAACTTTTTTCATTC ATTCCTCCATGATAAAATTTAA
B1663	3' end of *PflaB* fused to 5' end of *bbk32* coding sequence (forward primer)	TTAAATTTTATCATGGAGGAATGAATGA AAAAAGTTAAAAGTAAATATTTG
B1725	3' end of *bbk32* coding sequence (with NotI site) (reverse primer)	GCGGCCGCTTAGTACCAAACGCCATTC TTGTC
B1736	3' end of *PflaB* fused to 5' end of *revA* coding sequence (forward primer)	TTAAATTTTATCATGGAGGAATGAATGA GAAATAAAAACATATTTAAATTA
B1737	3' end of *PflaB* fused to 5' end of *revA* coding sequence (reverse primer)	TAATTTAAATATGTTTTTATTTCTCATTC ATTCCTCCATGATAAAATTTAA
B1747	3' end of *revA* coding sequence (with NotI site) (reverse primer)	GCGGCCGCTTAATTAGTGCCCTCTTCG AGGA
B1738	3' end of *revA* coding sequence fused to 5' end of *3Xflag* coding sequence (forward primer)	TCCTCGAAGAGGGCACTAATGACTACA AAGACCATGACGG
B1739	3' end of *revA* coding sequence fused to 5' end of *3Xflag* coding sequence (reverse primer)	CCGTCATGGTCTTTGTAGTCATTAGTGC CCTCTTCGAGGA
B1724	3' end of *3Xflag* coding sequence (with NotI site) (reverse primer)	GCGGCCGCCTACTTGTCATCGTCATCC TTGTA
B1728	3' end of *PflaB* fused to 5' end of *bb0347* coding sequence (forward primer)	TTAAATTTTATCATGGAGGAATGATTGA TAAAAAATGTCTTTGAATTACA
B1729	3' end of *PflaB* fused to 5' end of *bb0347* coding sequence (reverse primer)	TGTAATTCAAAGACATTTTTTATCAATCAT TCCTCCATGATAAAATTTAA
B1745	3' end of *bb0347* coding sequence (with NotI site) (reverse primer)	GCGGCCGCTTAGGTTTGATTTTTTATTT TTTTTATTA
B1730	3' end of *bb0347* coding sequence fused to 5' end of *3Xflag* coding sequence (forward primer)	CTAATAAAAAAAATAAAAAATCAAACCG ACTACAAAGACCATGACGG
B1731	3' end of *bb0347* coding sequence fused to 5' end of *3Xflag* coding sequence (reverse primer)	CCGTCATGGTCTTTGTAGTCGGTTTGAT TTTTTATTTTTTTTATTAG
B1732	3' end of *PflaB* fused to 5' end of *revB* coding sequence (forward primer)	TTAAATTTTATCATGGAGGAATGAATGC AAAAAATAAACATAGCTAAAT
B1733	3' end of *PflaB* fused to 5' end of *revB* coding sequence (reverse primer)	ATTTAGCTATGTTTATTTTTTGCATTCAT TCCTCCATGATAAAATTTAA
B1799	3' end of *revB* coding sequence (with NotI site) (reverse primer)	GCGGCCGCTTAATCTTCTTCAAGATATT TTATTATACTG
B1735	3' end of *revB* coding sequence fused to 5' end of *3Xflag* coding sequence (forward primer)	CCGTCATGGTCTTTGTAGTCATCTTCTT CAAGATATTTTATTATAC
B1734	3' end of *revB* coding sequence fused to 5' end of *3Xflag* coding sequence (reverse primer)	GTATAATAAAATATCTTGAAGAAGATGA CTACAAAGACCATGACGG
B1703	Forward primer used for sequencing and screening of pCE320-based constructs	GCTATGACCATGATTACGCC
B1704	Reverse primer used for sequencing and screening of pCE320-based constructs	GGGTTTTCCCAGTCACGAC

Primers used in this study, *continued*

Primer	Target	Sequence (5'-3')
B70	Forward primer used for PCR screening of pCE320-based constructs (amplifies *kan* resistance gene)	CATATGAGCCATATTCAACGGGAAACG
B71	Reverse primer used for PCR screening of pCE320-based constructs (amplifies *kan* resistance gene)	AAAGCCGTTTCTGTAATGAAGGAG
B1672	Forward primer for qPCR amplification of *flaB* DNA	GCAGCTAATGTTGCAAATCTTTTC
B1673	Reverse primer for qPCR amplification of *flaB* DNA	GCAGGTGCTGGCTGTTGA
RevAfp/ pQE30	Forward primer used for cloning *revA* coding sequence into pQE30	CGGGATCCTGTAAAGCATATGTAGAA
RevArp/ pQE30	Reverse primer used for cloning *revA* coding sequence into pQE30	CGGTCGACTTAATTAGTGCCCTCTTC
RevBfp/ pQE30	Forward primer used for cloning *revB* coding sequence into pQE30	CGGGATCCGAACTATTTATAATAAAA
RevBrp/ pQE30	Reverse primer used for cloning *revB* coding sequence into pQE30	CGGTCGACTTAATCTTCTTCAAGATA
BB0347fp/ pQE30	Forward primer used for cloning *bb0347* coding sequence into pQE30	CGGGATCCTCTTTGAATTACACTGAA
BB0347rp/ pQE30	Reverse primer used for cloning *bb0347* coding sequence into pQE30	CGGTCGACTTAGGTTTGATTTTTTAT

Table S4: Detailed statistical data (all figures)

Fig	Comparison	P-value
2B	**ANOVA**	**<0.0001**
	Pairwise comparisons (t-test):	
	Infectious vs *bbk32* KO	0.1837
	Infectious vs non-infectious	<0.0001
	bbk32 KO vs non-infectious	<0.0001
2C	**ANOVA**	**0.0006**
	Pairwise comparisons (t-test):	
	Infectious –FN-C/H II vs *bbk32* KO - FN-C/H II	0.0184
	Infectious – FN-C/H II vs infectious + FN-C/H II	0.0151
	Infectious – FN-C/H II vs *bbk32* KO + FN-C/H II	0.0102
	bbk32 KO – FN-C/H II vs infectious + FN-C/H II	0.7611
	bbk32 KO – FN-C/H II vs *bbk32* KO + FN-C/H II	0.5408
	Infectious + FN-C/H II vs *bbk32* KO + FN-C/H II	0.8202
3C	**ANOVA**	**0.0076**
	Pairwise comparisons (t-test):	
	BBK32 WT vs RevA	0.0331
	BBK32 WT vs BB0347	0.0758
	BBK32 WT vs RevB	0.0155
	BBK32 WT vs non-infectious	0.0064
	RevA vs non-infectious	0.1689
	BB0347 vs non-infectious	0.2525
	RevB vs non-infectious	0.5860
4C	**ANOVA**	**0.0033**
	Pairwise comparisons (t-test):	
	BBK32 WT vs BBK32 Δ45-68	0.9233
	BBK32 WT vs BBK32 Δ158-182	0.1046
	BBK32 WT vs non-infectious	0.0154
	BBK32 Δ45-68 vs BBK32 Δ158-182	0.0529
	BBK32 Δ45-68 vs non-infectious	0.0005
	BBK32 Δ158-182 vs non-infectious	0.2850
4D	**ANOVA**	**0.0021**
	Pairwise comparisons (t-test):	
	BBK32 WT vs BBK32 Δ45-68	0.1664
	BBK32 WT vs BBK32 Δ158-182	0.2131
	BBK32 WT vs non-infectious	0.0673
	BBK32 Δ45-68 vs BBK32 Δ158-182	0.7220
	BBK32 Δ45-68 vs non-infectious	0.0866
	BBK32 Δ158-182 vs non-infectious	0.0902
4E	**ANOVA**	**0.0103**
	Pairwise comparisons (t-test):	
	BBK32 WT vs BBK32 Δ45-68	0.0734
	BBK32 WT vs BBK32 Δ158-182	0.2937
	BBK32 WT vs non-infectious	0.0622
	BBK32 Δ45-68 vs BBK32 Δ158-182	0.0048
	BBK32 Δ45-68 vs non-infectious	0.8095
	BBK32 Δ158-182 vs non-infectious	0.0426
S2A	**ANOVA**	**0.1613**
	Pairwise comparisons (t-test):	
	Infectious vs BBK32 WT	0.8698
	Infectious vs RevA	0.2624

Table S4: Detailed statistical data, *continued*

Fig	Comparison	P-value
S2A	Pairwise comparisons (t-test):	
	Infectious vs BB0347	0.2709
	Infectious vs RevB	0.4945
	Infectious vs non-infectious	0.1889
	BBK32 WT vs RevA	0.2574
	BBK32 WT vs BB0347	0.3209
	BBK32 WT vs RevB	0.5440
	BBK32 WT vs non-infectious	0.1929
	RevA vs non-infectious	0.3899
	BB0347 vs non-infectious	0.3298
	RevB vs non-infectious	0.2595
S2B	**ANOVA**	**<0.0001**
	Pairwise comparisons (t-test):	
	Infectious vs BBK32 WT	0.6163
	Infectious vs RevA	0.0019
	Infectious vs BB0347	0.0011
	Infectious vs RevB	0.0021
	Infectious vs non-infectious	0.0006
	BBK32 WT vs RevA	0.0116
	BBK32 WT vs BB0347	0.0090
	BBK32 WT vs RevB	0.0129
	BBK32 WT vs non-infectious	0.0068
	RevA vs non-infectious	0.4179
	BB0347 vs non-infectious	0.5258
	RevB vs non-infectious	0.2397
S2C	**ANOVA**	**<0.0001**
	Pairwise comparisons (t-test):	
	Infectious vs BBK32 WT	0.5695
	Infectious vs RevA	<0.0001
	Infectious vs BB0347	<0.0001
	Infectious vs RevB	0.0003
	Infectious vs non-infectious	<0.0001
	BBK32 WT vs RevA	0.0027
	BBK32 WT vs BB0347	0.0017
	BBK32 WT vs RevB	0.0109
	BBK32 WT vs non-infectious	0.0017
	RevA vs non-infectious	0.5541
	BB0347 vs non-infectious	0.9893
	RevB vs non-infectious	0.0302
S3A	**ANOVA**	**0.0003**
	Pairwise comparisons (t-test):	
	Infectious vs BBK32 WT	0.8767
	Infectious vs BBK32 Δ45-68	0.6691
	Infectious vs BBK32 Δ158-182	0.8917
	Infectious vs non-infectious	0.0436
	BBK32 WT vs BBK32 Δ45-68	0.7206
	BBK32 WT vs BBK32 Δ158-182	0.7429
	BBK32 WT vs non-infectious	0.0082
	BBK32 Δ45-68 vs BBK32 Δ158-182	0.5260
	BBK32 Δ45-68 vs non-infectious	<0.0001
	BBK32 Δ158-182 vs non-infectious	0.0261

Table S4: Detailed statistical data, *continued*

Fig	Comparison	P-value
S3B	**ANOVA**	**<0.0001**
	Pairwise comparisons (t-test):	
	Infectious vs BBK32 WT	0.4666
	Infectious vs BBK32 Δ45-68	0.0186
	Infectious vs BBK32 Δ158-182	0.2226
	Infectious vs non-infectious	0.0015
	BBK32 WT vs BBK32 Δ45-68	0.0117
	BBK32 WT vs BBK32 Δ158-182	0.6090
	BBK32 WT vs non-infectious	0.0020
	BBK32 Δ45-68 vs BBK32 Δ158-182	0.0122
	BBK32 Δ45-68 vs non-infectious	0.0323
	BBK32 Δ158-182 vs non-infectious	0.0035
S3C	**ANOVA**	**0.1363**
	Pairwise comparisons (t-test):	
	Infectious vs BBK32 WT	0.8728
	Infectious vs BBK32 Δ45-68	0.2066
	Infectious vs BBK32 Δ158-182	0.6678
	Infectious vs non-infectious	0.1889
	BBK32 WT vs BBK32 Δ45-68	0.2116
	BBK32 WT vs BBK32 Δ158-182	0.7248
	BBK32 WT vs non-infectious	0.1948
	BBK32 Δ45-68 vs BBK32 Δ158-182	0.3581
	BBK32 Δ45-68 vs non-infectious	0.3479
	BBK32 Δ158-182 vs non-infectious	0.3463

Supplemental References

Eggers, C. H., M. J. Caimano, M. L. Clawson, W. G. Miller, D. S. Samuels & J. D. Radolf, (2002) Identification of loci critical for replication and compatibility of a *Borrelia burgdorferi* cp32-based shuttle vector for the expression of fluorescent reporters in the Lyme disease spirochete. *Molecular microbiology* **43**: 281-295.

Fischer, J. R., K. T. Leblanc & J. M. Leong, (2006) Fibronectin binding protein BBK32 of the Lyme disease spirochete promotes bacterial attachment to glycosaminoglycans. *Infection and immunity* **74**: 435-441.

Lee, W. Y., T. J. Moriarty, C. H. Wong, H. Zhou, R. M. Strieter, N. van Rooijen, G. Chaconas & P. Kubes, (2010) An intravascular immune response to *Borrelia burgdorferi* involves Kupffer cells and iNKT cells. *Nature immunology* **11**: 295-302.

Lin, Y.-P., Q. Chen, N. P. Dufour, J. R. Fischer & J. M. Leong, (2012) *Borrelia burgdorferi* BBK32is a bifunctional adhesin with glycosaminoglycan- and fibronectin-binding activities that each confer binding to distinct mammalian cell types. *Manuscript in preparation*.

Moriarty, T. J., M. U. Norman, P. Colarusso, T. Bankhead, P. Kubes & G. Chaconas, (2008) Real-time high resolution 3D imaging of the lyme disease spirochete adhering to and escaping from the vasculature of a living host. *PLoS pathogens* **4**: e1000090.

Seshu, J., M. D. Esteve-Gassent, M. Labandeira-Rey, J. H. Kim, J. P. Trzeciakowski, M. Hook & J. T. Skare, (2006) Inactivation of the fibronectin-binding adhesin gene *bbk32* significantly attenuates the infectivity potential of *Borrelia burgdorferi*. *Molecular microbiology* **59**: 1591-1601.

Wu, J., E. H. Weening, J. B. Faske, M. Hook & J. T. Skare, (2011) Invasion of eukaryotic cells by *Borrelia burgdorferi* requires □1 integrins and Src kinase activity. *Infection and immunity* **79**: 1338-1348.

Zeghouf, M., J. Li, G. Butland, A. Borkowska, V. Canadien, D. Richards, B. Beattie, A. Emili & J. F. Greenblatt, (2004) Sequential Peptide Affinity (SPA) system for the identification of mammalian and bacterial protein complexes. *J Proteome Res* **3**: 463-468.

Figure S1

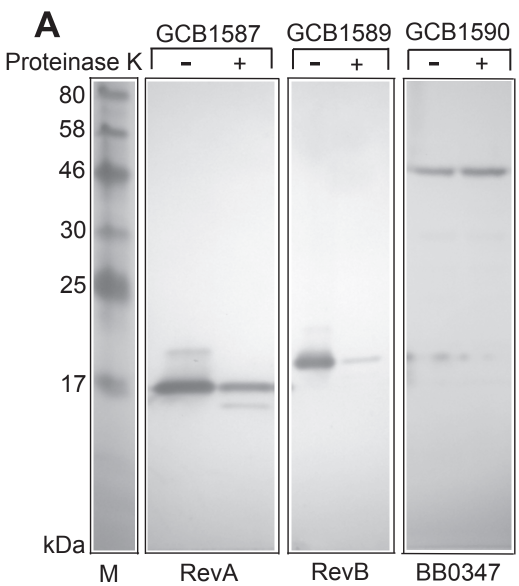

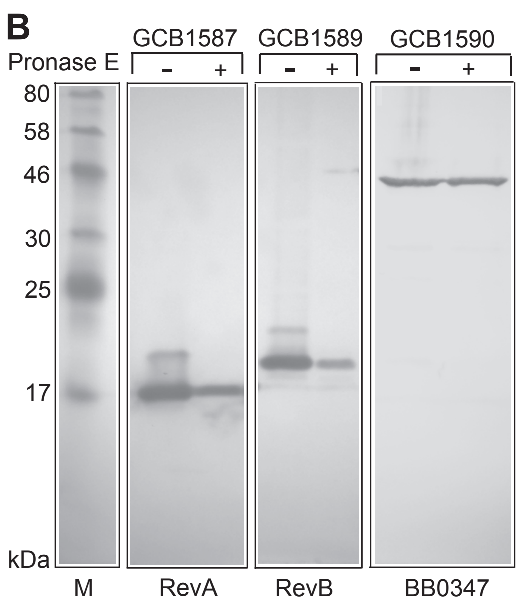

Figure S1: Adhesin expression and localization in gain of function strains. *B. burgdorferi* (pellets from $5x10^7$ - $1x10^8$ spirochetes) in 100 µl were incubated in the absence or presence of proteinase K (**A**) or pronase (**B**) as previously described (Probert & Johnson, 1998, Fischer et al., 2006, Norman *et al.*, 2008). The concentration of proteinase K used in the gel shown was 400 µg/ml for all proteins and the concentration of pronase used was 600 µg/ml for RevA and RevB and 2 mg/ml for BB0347. For RevA (19 kDa) and RevB (21 kDa), $1.25x10^7$ lysed bacteria were loaded per lane. For BB0347 (56 kDa) $5x10^7$ lysed spirochetes were loaded.

Figure S2

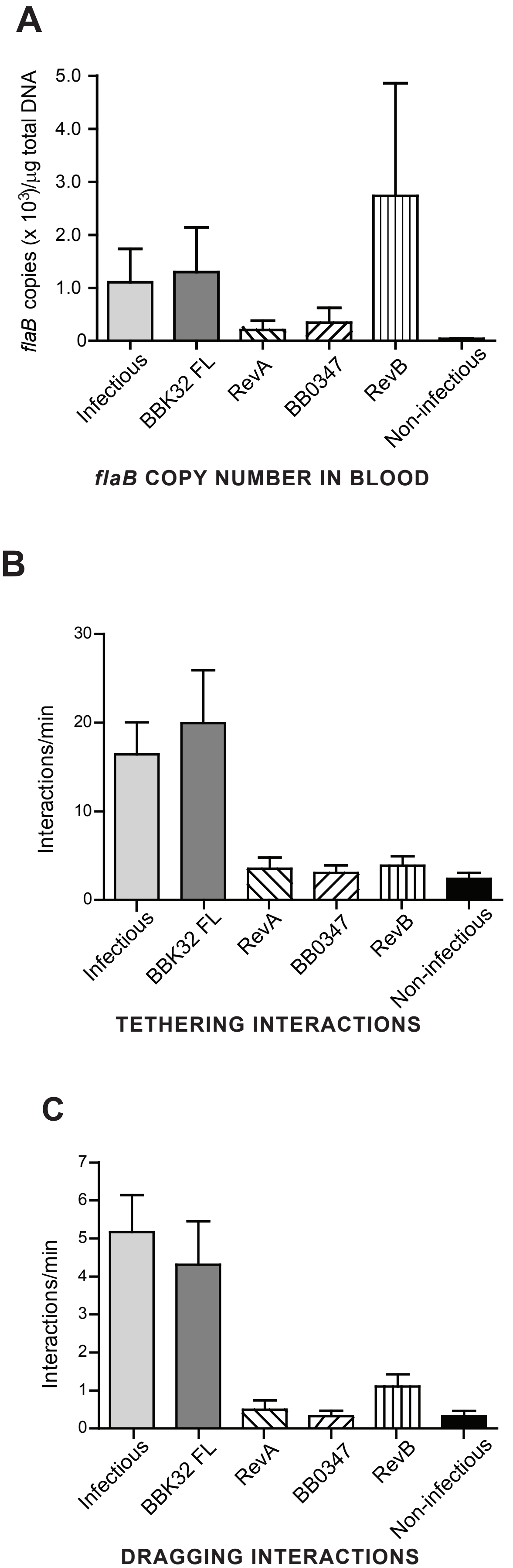

Figure S2: Role of BBK32 and other *B. burgdorferi* Fn-binding proteins in microvascular interactions *in vivo* and in evasion of intravascular immune clearance. Unadjusted data from the experiments presented in **Fig. 3B. A)** Relative numbers of circulating bacteria for four fluorescent *B. burgdorferi* gain-of-function strains expressing full-length BBK32 (BBK32 FL), RevA, BB0347 or RevB, and infectious and non-infectious controls. **Strains:** 1) GCB726: infectious B31 5A4 NP1 control (infectious), 2) GCB1585: non-infectious expressing full-length BBK32 *in trans* (BBK32 FL), 3) GCB1570: non-infectious expressing RevA *in trans* (RevA), 4) GCB1574: non-infectious expressing BB0347 *in trans* (BB0347), 5) GCB1586: non-infectious expressing RevB *in trans*, and 6) GCB706: non-infectious parent, B31-A. Spirochete burden in blood was measured by qPCR amplification of *flaB* sequences, and *flaB* copy number was normalized to total number of µg of DNA isolated from each blood sample. Blood samples were collected from the same mice where microvascular interactions had previously been examined by intravital microscopy, an average of 1 hour following intravenous inoculation (see **Panels B-C** below). N=4 mice inoculated with infectious *B. burgdorferi*; n=6 BBK32 FL; n=6 RevA; n=5 BB0347; n=6 RevB; n=4 non-infectious. Means and standard error bars are indicated for each experimental group. **B-C)** Microvascular interaction rates (**B**: tethering interactions; **C** dragging interactions) for *B. burgdorferi* gain-of-function strains expressing full-length BBK32 (BBK32 FL; strain GCB1585), RevA (strain GCB1570), BB0347 (strain GCB1574) or RevB (strain GCB1586), and infectious and non-infectious controls (strains GCB726 and GCB706, respectively), as analyzed by high acquisition rate spinning disk confocal intravital microscopy. Statistical testing for

Figure S3

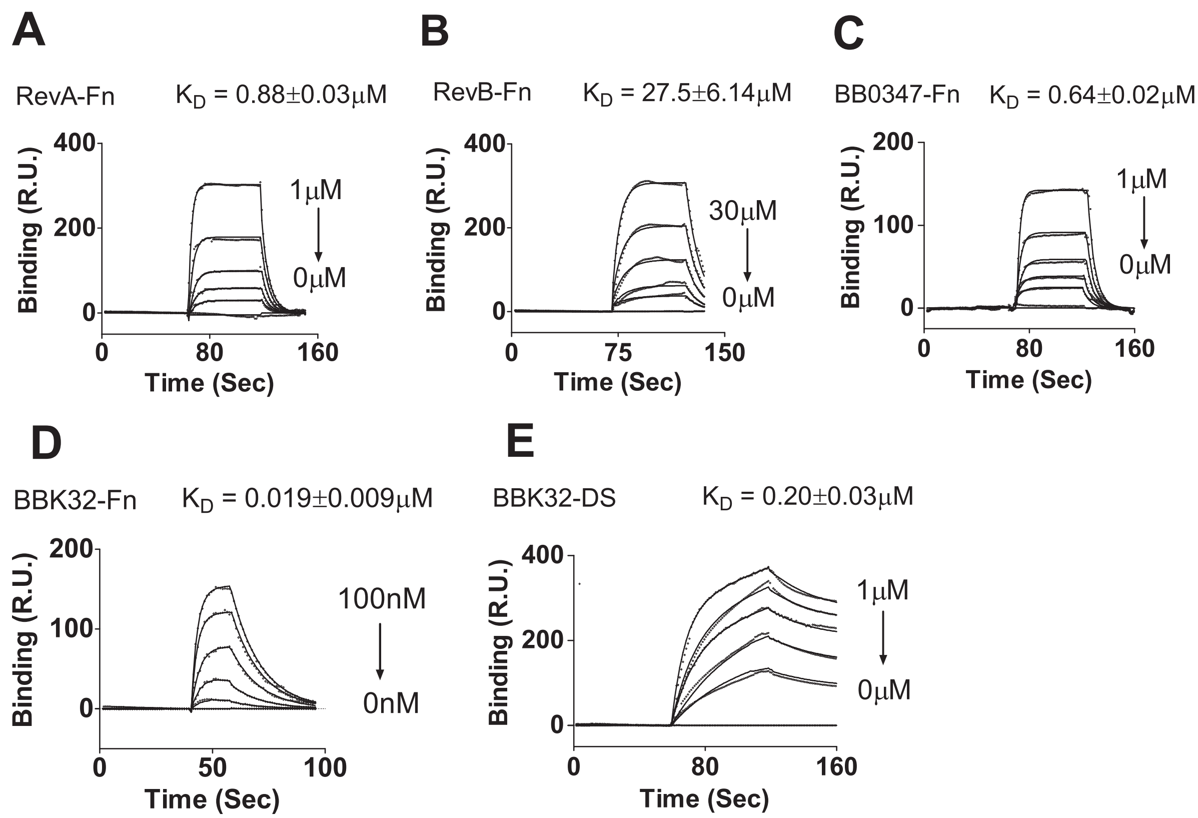

Figure S3: Quantitative surface plasmon resonance (SPR) analysis of BBK32, RevA, RevB and BB0347 interactions with Fn and dermatan sulfate. For SPR analysis of Fn binding, 1 µg of Fn was immobilized on the surface of a CM5 chip. A range of concentrations of **(A)** RevA (0, 0.0625, 0.125, 0.25, 0.5, 1 µM), of **(B)** RevB (0, 1.875, 3.75, 7.5, 15, 30 µM), of **(C)** BB0347 (0, 0.0625, 0.125, 0.25, 0.5, 1 µM), or of **(D)** BBK32 (0, 6.25, 12.5, 25, 50, 100 nM) in PBS buffer at pH 7.5 were passed over the chip. **(E)** To measure the affinity of BBK32 for dermatan sulfate (DS), 1µg of biotinylated DS was immobilized on the surface of an SA chip. Various concentrations of BBK32 (0, 0.0625, 0.125, 0.25, 0.5, 1 µM) in PBS buffer at pH 7.5 were circulated over the chip. The K_D, K_{on} and K_{off} were obtained from the average of triplicate experiments and are shown in **Table 1**.

Figure S4

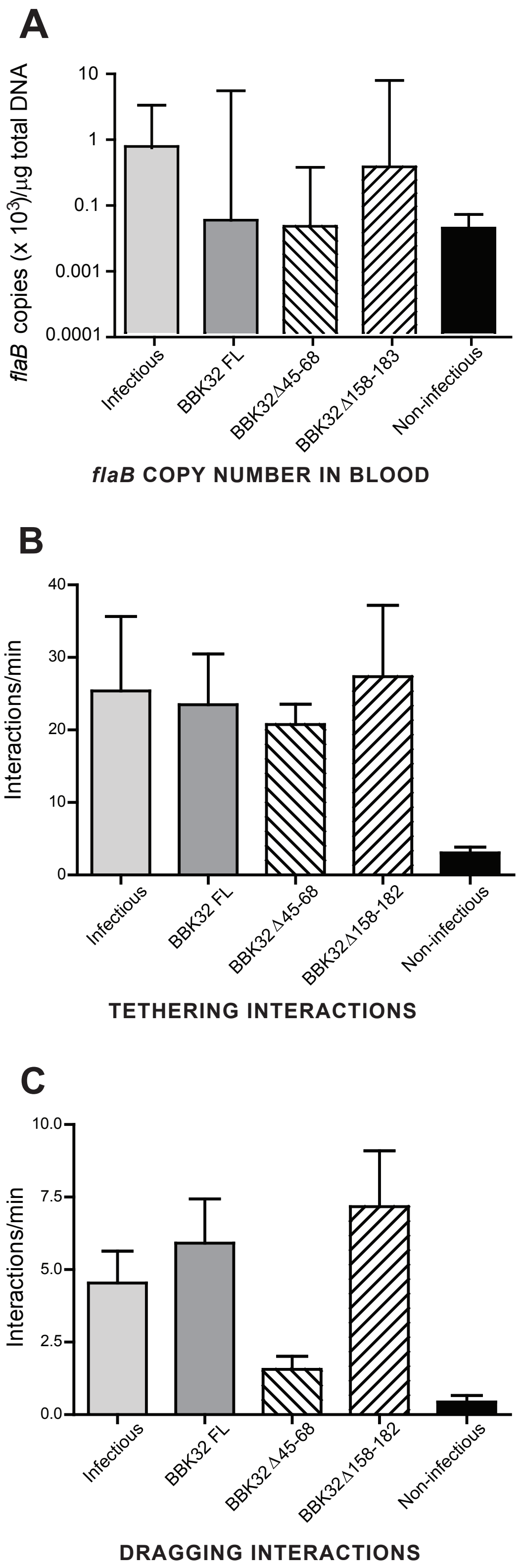

Figure S4: Unadjusted data for the microvascular interaction experiments presented in Fig. 5. A) Relative numbers of circulating bacteria for the experiment shown in **Fig. 5. B)** Tethering interaction rates. **C)** Dragging interaction rates. The data shown is without normalization to *flaB* copy number. Spirochete burden in blood was measured by qPCR amplification of *flaB* sequences, and *flaB* copy number was normalized to total number of μg of DNA isolated from each blood sample. Blood samples were collected from the same mice where microvascular interactions had previously been examined by intravital microscopy, an average of 1 hour following intravenous inoculation (see **Fig. 5**). Means and standard error bars are indicated for each experimental group in panels **A** and **B**. Panel **C** shows medians and ranges for each experimental group. Statistical testing for significant differences among all experimental groups was performed using a non-parametric Kruskal-Wallis ANOVA (P values of 0.0.0003, <0.0001 and 0.1363 for **A**, **B** and **C**, respectively). All statistical data may be found in **Table S4**.